Cancer Biology Publications and Presentations   Molecular, Cell and Cancer Biology

2014-05-08

Regulated splicing of the alpha6 integrin cytoplasmic domain determines the fate of breast cancer stem cells

Hira Lal Goel
University of Massachusetts Medical School

Et al.

Let us know how access to this document benefits you.

Repository Citation

Regulated Splicing of the α6 Integrin Cytoplasmic Domain Determines the Fate of Breast Cancer Stem Cells

Hira Lal Goel,[1] Tatiana Gritsko,[1] Bryan Pursell,[1] Cheng Chang,[1] Leonard D. Shultz,[2] Dale L. Greiner,[3] Jens Henrik Norum,[4] Rune Toftgard,[4] Leslie M. Shaw,[1] and Arthur M. Mercurio[1,*]
[1]Department of Cancer Biology, University of Massachusetts Medical School, Worcester, MA 01605, USA
[2]The Jackson Laboratory, Bar Harbor, ME 04609, USA
[3]Program in Molecular Medicine, University of Massachusetts Medical School, Worcester, MA 01605, USA
[4]Department of Bioscience and Nutrition, Center for Biosciences, Karolinska Institute, Novum, 14183 Huddinge, Sweden
*Correspondence: arthur.mercurio@umassmed.edu
http://dx.doi.org/10.1016/j.celrep.2014.03.059

SUMMARY

Although the α6β1 integrin has been implicated in the function of breast and other cancer stem cells (CSCs), little is known about its regulation and relationship to mechanisms involved in the genesis of CSCs. We report that a CD44^{high}/CD24^{low} population, enriched for CSCs, is comprised of distinct epithelial and mesenchymal populations that differ in expression of the two α6 cytoplasmic domain splice variants: α6A and α6B. α6Bβ1 expression defines the mesenchymal population and is necessary for CSC function, a function that cannot be executed by α6A integrins. The generation of α6Bβ1 is tightly controlled and occurs as a consequence of an autocrine vascular endothelial growth factor (VEGF) signaling that culminates in the transcriptional repression of a key RNA-splicing factor. These data alter our understanding of how α6β1 contributes to breast cancer, and they resolve ambiguities regarding the use of total α6 (CD49f) expression as a biomarker for CSCs.

INTRODUCTION

Most solid tumors, including breast carcinomas, harbor a relatively small population of cells with characteristics of stem cells, including the ability to self-renew and populate new tumors. This population is often referred to as tumor-initiating cells or cancer stem cells (CSCs) (Al-Hajj et al., 2003; Baccelli and Trumpp, 2012; Visvader and Lindeman, 2012). Understanding the biology of CSCs is highly significant because this population of cells is likely responsible for tumor recurrence in response to therapy and it may contribute to metastasis (Calcagno et al., 2010; Dean et al., 2005; Pinto et al., 2013). A frequent observation is that high expression of the α6 integrin subunit (CD49f) is a biomarker for breast and other CSCs (Goel et al., 2013; Meyer et al., 2010; Vieira et al., 2012). This subunit heterodimerizes

with either the β1 or β4 subunits to generate the α6β1 and α6β4 integrins, which function primarily as laminin receptors (Mercurio, 1990). Interestingly, however, the β4 subunit appears to be expressed at very low levels, if at all, in CSCs compared to non-CSCs, indicating that α6β1 is the dominant α6 integrin expressed by CSCs (Goel et al., 2013; Lathia et al., 2010). Although the α6β1 integrin has been implicated in the function of breast and other CSCs (Cariati et al., 2008; Goel et al., 2013; Lathia et al., 2010), much needs to be learned about the contribution of this integrin to the genesis of CSCs. Specifically, α6β1 is expressed in both differentiated (e.g., luminal) and dedifferentiated breast carcinoma cells (e.g., triple-negative [TPN]) and the relationship between α6β1 and differentiation status is unclear, especially in the context of CSCs. There are also reports that high α6β1 expression is not always characteristic of CSCs (Sarrio et al., 2012). The fact that the α6 integrin exists as two distinct cytoplasmic domain variants, α6A and α6B, which are generated by alternative mRNA splicing (Hogervorst et al., 1991; Tamura et al., 1991), could be relevant to our understanding of the function of this integrin in CSCs, but little is known about the relative contribution of these variants to self-renewal and tumor initiation.

This study was prompted by our analysis of the CD44^{high}/CD24^{low} population of breast cancer cells, a minor population known to be tumorigenic and enriched for stem cell properties (Al-Hajj et al., 2003; Azzam et al., 2013; Iliopoulos et al., 2011). Unexpectedly, we discovered that this population is comprised of distinct epithelial and mesenchymal populations and that these populations differ in their expression of the α6A and α6B integrin subunits. The epithelial population is characterized by predominantly α6A and very low levels of α6B expression, and α6B expression predominates in the mesenchymal population. This observation prompted us to investigate the relevance of α6A and α6B expression to self-renewal and tumor initiation. We discovered that the α6Bβ1 integrin is the critical α6β1 variant that drives CSC function in TPN breast cancer and promotes tumor initiation and that this function cannot be executed by α6A integrins. Given that splicing regulates the differential expression of α6A and α6B, we discovered that α6Bβ1 expression is sustained by a vascular endothelial growth factor
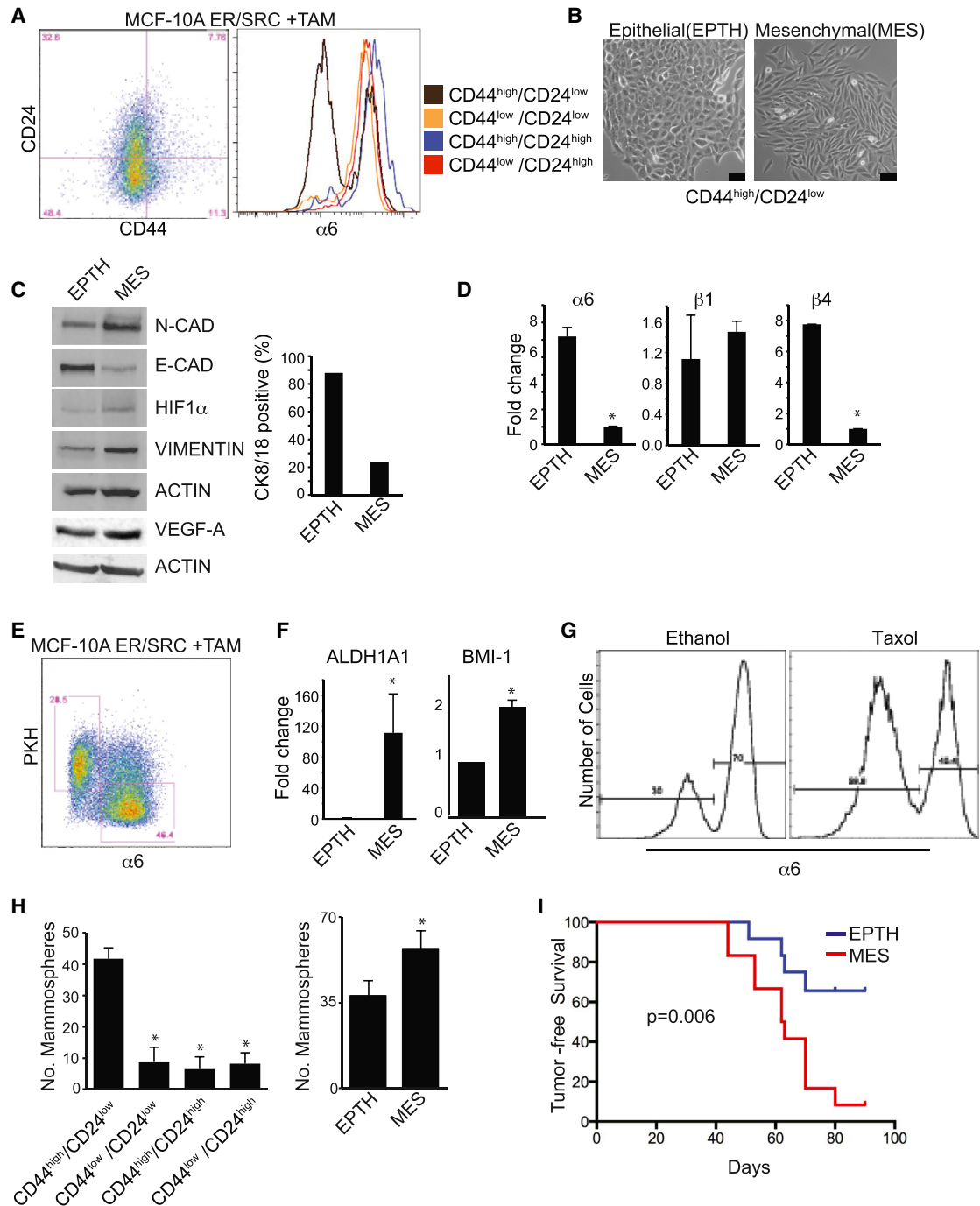
Figure 1. Identification of Distinct CD44^high^CD24^low^ Populations that Differ in Morphology and Stem Cell Properties

(A) MCF-10A ER-SRC cells were treated with 4-hydroxytamoxifen (TAM) and FACS analyzed using CD44, CD24, and α6 (GoH3) antibodies.

(B) The CD44^high^/CD24^low^ population isolated from TAM-treated MCF-10A ER-SRC cells was sorted by FACS into two subpopulations based on expression of the α6 integrin subunit. Photomicrographs of these two subpopulations designated as EPTH (α6 high) and MES (α6 low) are shown. The scale bar represents 100 μm.

(C) Cell extracts from EPTH and MES cells were immunoblotted to assess expression of N-cadherin, E-cadherin, HIF-1α, vimentin, actin, and VEGF-A (left panel). EPTH and MES cells were immunostained for CK8 and CK18, and the quantitation of positive cells is presented (right panel).

(D) Expression of integrin α6, β1, and β4 mRNAs was quantified in EPTH and MES cells using qPCR.

(E) The CD44^high^/CD24^low^ population from TAM-treated MCF-10A ER-SRC cells was stained with PKH26 and cultured for 14 days. Cells were analyzed by FACS for PKH and integrin α6 expression.

(F) Expression of ALDH1A1 and BMI-1 mRNAs was quantified in EPTH and MES cells using qPCR.

(legend continued on next page)

(VEGF)-signaling pathway that promotes dedifferentiation and culminates in the repression of a key splicing factor that impedes the genesis of α6B. These data reveal an integrated pathway that regulates integrin splicing and the consequent formation of an α6 splice variant necessary for self-renewal and tumor initiation.

RESULTS

Identification of Two Distinct Populations of CD44^{high}/CD24^{low} Cells that Differ in Stem Cell Properties and Expression of α6 Integrin Splice Variants

Expression of SRC in MCF-10A cells using a tamoxifen-inducible ER-SRC construct increases the number of CD44^{high}/CD24^{low} cells when compared with nontransformed cells (Iliopoulos et al., 2011). Flow cytometry using an α6-specific antibody (Ab) revealed two distinct populations of cells within the CD44^{high}/CD24^{low} population that differ in their relative expression of α6: populations of relative high and low α6 expression. In contrast, only the high α6 peak was seen in the other, non-CSC subpopulations (CD44^{low}CD24^{low}, CD44^{high}CD24^{high}, and CD44^{low}CD24^{high}; Figure 1A). Moreover, SRC transformation alters the distribution of α6 expression with a shift toward the α6-low peak (Figure S1A). To gain insight into the nature of these two α6 populations, we sorted CD44^{high}/CD24^{low} cells with fluorescence-activated cell sorting (FACS) in order to isolate the α6-high and low cells and characterized them. Surprisingly, these two populations differed markedly in their morphology. The α6-low population had a distinct mesenchymal morphology (MES) compared to the epithelial morphology (EPTH) of the α6-high population (Figure 1B). Consistent with their morphology, EPTH cells express more E-cadherin and MES cells express more N-cadherin, vimentin, hypoxia-inducible factor 1α (HIF-1α), and VEGF. Cytokeratin 8 and cytokeratin 18, markers of differentiated secretory epithelia, are enriched in the EPTH population (Figure 1C). Snai1 and Zeb1, epithelial-mesenchymal transition (EMT)-associated transcription factors (Nieto and Cano, 2012), are expressed in the MES population (Figure S1B). Also, expression of the β4 integrin subunit is high in EPTH cells and low in MES cells, indicating that EPTH cells express primarily α6β4 and MES express α6β1 (Figure 1D). We also observed that EPTH cells are stable and maintain their epithelial nature in culture but that MES cells slowly transition to epithelial cells (Figure S1C).

Although the CD44^{high}/CD24^{low} population is considered to have stem cell properties (Al-Hajj et al., 2003; Azzam et al., 2013; Iliopoulos et al., 2011), our data indicate that this population is heterogeneous and that the EPTH and MES populations may differ in stem cell characteristics. Indeed, we observed increased expression of ALDH1 and BMI1, which are established stem cell markers (Douville et al., 2009; Liu et al., 2006), and increased retention of PKH, a marker for slow-cycling cells

(Pece et al., 2010), in the MES population (Figures 1E and 1F). To substantiate these results, we treated SRC-transformed MCF-10A cells with Taxol, which selectively kills growing cells and enriches for slow-cycling cells (Tanei et al., 2009). Taxol treatment enriched cells in the first peak of α6 integrin (MES cells), supporting the hypothesis that these are slow-cycling cells (Figure 1G). Most importantly, the EPTH and MES cells exhibited significant differences in their ability to form mammospheres (Figures 1H and S1D) and initiate tumors upon mammary fat pad implantation in nonobese diabetic (NOD).Cg-Prkdc[scid] IL2rg[tm1Wjl] (NSG) mice (Figure 1I), indicating that the MES population is enriched for CSCs.

The fact that MES population exhibited reduced α6 integrin expression but enhanced CSC properties compared to the EPTH population prompted us to assess the relative expression of the α6A and α6B splice variants. We observed that EPTH cells express predominantly α6A and very low levels of α6B and that α6B is the predominant variant in the MES population (Figure 2A). Based on this result, we evaluated the relative expression of these variants in normal (MCF-10A), luminal (T47D and SK-BR-3), and TPN (MDA-MB-435, MD-MB-231, and SUM1315) breast cancer cell lines. Normal and luminal cell lines tested expressed predominantly α6A and TPN cells expressed predominantly α6B as detected by immunoblotting (Figure 2B).

The α6Bβ1 Integrin Promotes the Function of Breast CSCs, and Its Expression Is Tightly Regulated by Epithelial Splicing Factor ESRP1

To investigate the relative contribution of the α6Aβ1 and α6Bβ1 integrins, we used TPN breast cancer lines, which are enriched with CSCs. Given that these cells predominantly express α6B but also some α6A, we sought to obtain equivalent surface expression of α6Aβ1 and α6Bβ1. Also, it is not possible to design small hairpin RNAs (shRNAs) that target α6B specifically because of sequence homology between the two variants. For these reasons, we used an shRNA that targets the 3′ UTR that is common to both α6A and α6B to deplete the expression of endogenous α6 integrins, and then we re-expressed either α6A or α6B (Figures S2A and 2C). The cell lines generated predominantly express only one of these cytoplasmic variants (Figure 2C), and these two integrin variants exhibit similar levels of surface expression (Figure S2B). Cells expressing α6Bβ1 had decreased E-cadherin and increased vimentin expression and proliferated more slowly compared to cells expressing α6Aβ1 (Figures S2C and S2D). Also, compared to cells expressing either empty vector or α6Aβ1, cells expressing α6Bβ1 had significantly more self-renewal ability as measured by mammosphere serial passage (Figures 2D, S2E, and S2F), more retention of PKH (Figure S3A), and increased anchorage-independent growth (Figures 2E and S2G). To test whether tumor cell populations that express α6Bβ1 have a greater number of CSCs

(G) The CD44^{high}/CD24^{low} population isolated from TAM-treated MCF-10A ER-SRC cells was treated with either Taxol or ethanol for 7 days, and integrin α6 surface expression was analyzed by FACS.

(H) TAM- treated MCF-10A ER-SRC cells were FACS sorted into subpopulations based on expression of CD44 and CD24 and assayed for mammosphere formation (left panel). EPTH and MES cells were assayed for mammosphere formation (right panel).

(I) EPTH and MES cells (10^6 cells per mouse) were implanted in the mammary fat pads of NSG mice (n = 12), and tumor formation was assessed by palpation. The curve comparison was done using log rank test (p = 0.006).
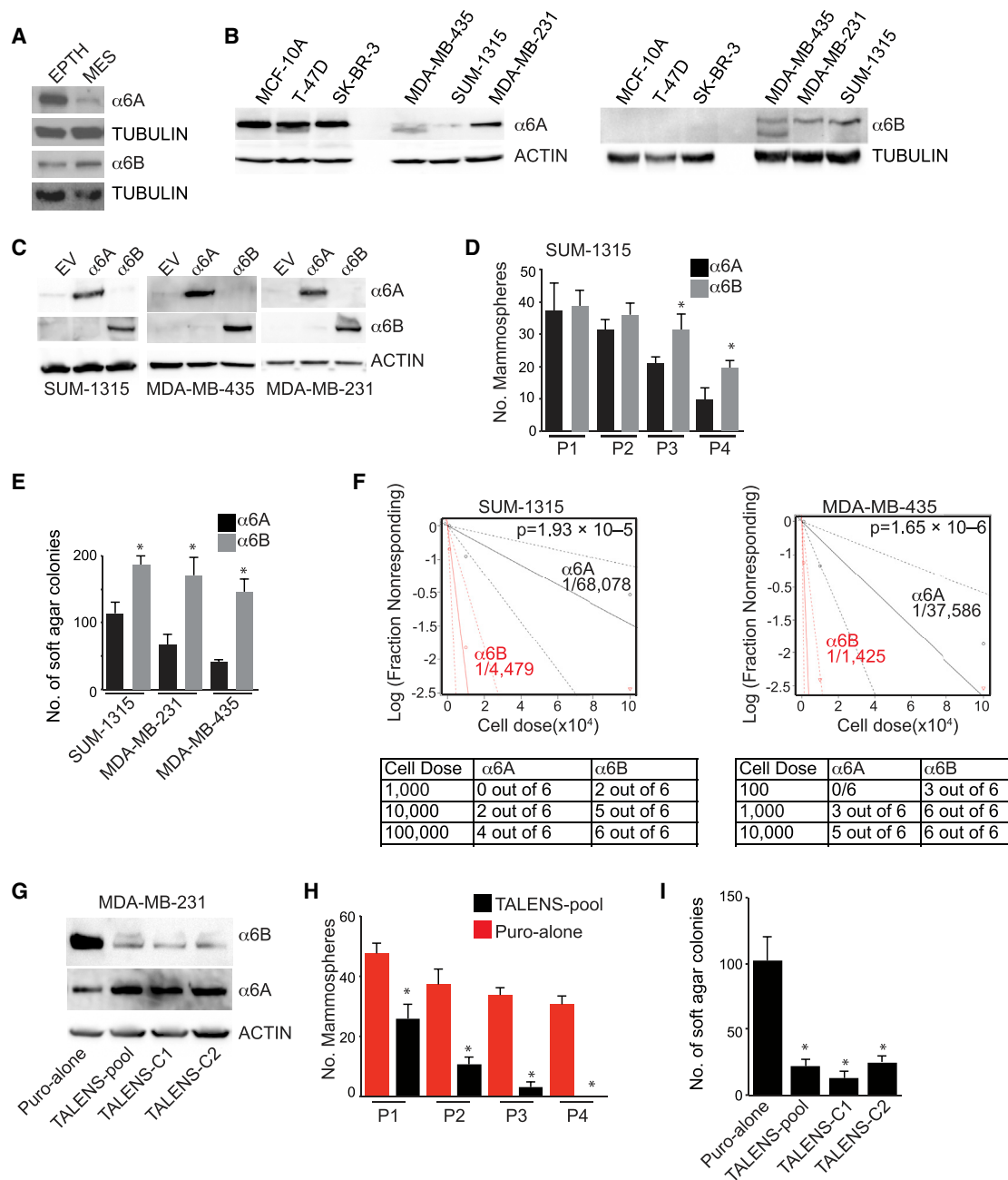
Figure 2. α6B Cytoplasmic Variant Expression Determines Tumor-Initiating Potential in Breast Cancer Cells

(A) Cell extracts from EPTH and MES were immunoblotted for integrin α6A, α6B, and tubulin.

(B) Cell extracts from breast cancer cell lines were immunoblotted for α6A (left blot) and α6B (right blot).

(C) Integrin α6-depleted SUM1315, MDA-MB-435, and MDA-MB-231 cells were stably transfected with either empty vector (EV), α6A, or α6B. Transfectants were analyzed by immunoblotting using α6A, α6B, or actin Abs.

(D) Mammospheres from SUM1315 transfectants (α6A or α6B) were passaged serially, and the number of mammospheres is presented.

(E) Integrin α6A and α6B transfectants of SUM1315, MDA-MB-435, and MDA-MB-231 cell lines were assessed for growth in soft agar.

(F) Integrin α6A and α6B transfectants of SUM1315 (left panel) and MDA-MB-435 (right panel) cells were transplanted into mammary fat pads of NSG mice using 10-fold serial dilution. The formation of palpable tumors was used to evaluate tumor initiation. Data are presented as a log-log plot, and frequency of stem cells is calculated by extreme limiting dilution analysis. Red, SUM1315-α6B (1/4,479) or MDA-MB-435-α6B (1/1,425); black, SUM1315-α6A (1/68,078) or MDA-MB-435-α6A (1/37,586).

(G) Expression of α6B was depleted in MDA-MB-231 cells using α6B-specific TALENs in combination with a donor plasmid containing a puromycin expression cassette, and expression of α6A, α6B, and actin was assessed by immunoblotting.

(H) Mammospheres from the transfectants in G (Puro-alone or TALENs-pool) were passaged serially, and the number of mammospheres is presented.

(I) Soft agar growth from the transfectants in G (Puro-alone, TALENs-pool, TALENs-C1, and TALENs-C2) is presented as the mean number of colonies in 20 fields.

compared to cells that express α6Aβ1, we performed limiting dilution experiments in vivo. As few as 100 cells for MDA-MB-435-α6B (three out of six mice) and 1,000 cells for SUM1315-α6B (two out of six mice) were sufficient for tumor initiation, whereas no tumor formation was observed by the corresponding number of α6A transfectants. Based on the limiting dilution assay, the frequency of CSCs was calculated to be approximately 1/1,425 (MDA-MB-435-α6B), 1/37,586 (MDA-MB-435-α6A), 1/4,479 (SUM1315-α6B), and 1/68,078 (SUM1315-α6A; Figure 2F). These data demonstrate that breast cancer cells expressing α6Bβ1 are significantly more enriched in stem cell properties than cells expressing α6Aβ1.

We made use of transcription activator-like effector nucleases (TALENs) to disrupt the alternative splicing site in the α6 integrin mRNA as a rigorous approach to substantiate the role of α6B and to circumvent the fact that RNAi cannot be used to target this splice variant specifically. TALEN-mediated disruption of the alternative splicing site resulted in markedly reduced α6B expression and a concomitant increase in α6A expression (Figure 2G). Importantly, depletion of α6B significantly inhibited self-renewal (Figure 2H) and colony formation in soft agar (Figure 2I).

Differential expression of α6A and α6B is determined by alternative splicing of the α6 subunit, a process mediated by specific splicing factors (Warzecha et al., 2010). We compared EPTH and MES cells for the expression of splicing factors (ESRP1, ESRP2, RBFOX2, and MBNL) that have been implicated in epithelial differentiation/EMT and CSCs and that could regulate α6 splicing (Brown et al., 2011; Shapiro et al., 2011; Yae et al., 2012; Han et al., 2013). ESRP1 is the only factor that exhibited a marked difference in expression between the two populations (24-fold lower in MES compared to EPTH cells; Figure 3A). The other factors are expressed at low levels in both populations (Figure 3A). Also, expression of ESRP1 is extremely low in TPN compared to luminal (MCF7) or normal (MCF-10A) breast cancer cells (Figure 3B). Based on these observations, we hypothesized that loss of ESRP1 increases α6B and decreases α6A. Indeed, downregulation of ESRP1 in SRC-transformed MCF-10A cells significantly increased α6B and reduced α6A expression (Figure 3C). Similarly, exogenous expression of ESRP1 in TPN MDA-MB-435, SUM1315, MDA-MB-231, and SUM159 cells increased α6A and reduced α6B expression, and it diminished the ability of these cells to form colonies in soft agar (Figures 3D, 3E, and S3B). Downregulation of ESRP1 significantly increased the number of soft agar colonies and self-renewal ability (Figure S3C). Taxol treatment of SRC-transformed MCF-10A cells, which enriches for CSCs (Tanei et al., 2009), increased α6B expression and reduced expression of ESRP1 and α6A (Figure 3F). Expression of ESRP1 in TPN cell lines reduced their self-renewal potential as measured by serial passaging of mammospheres (Figure 3G).

To assess whether the correlation between α6 integrin variants and ESRP1 exists in clinical samples from breast cancer patients, we quantified ESRP1, α6A, and α6B mRNA expression in TPN and non-TPN breast tumor samples. VEGF expression was also quantified in the same samples because we previously reported that VEGF is highly expressed in TPN samples compared to non-TPN (Goel et al., 2013). As shown in Figures 4A and 4B, expression of α6A, as well as ESRP1, is significantly lower in TPN compared to non-TPN tumors. In contrast, VEGF and α6B expression is significantly higher in TPN samples. We also observed that ESRP1 is positively correlated with α6A but negatively correlated with VEGF and α6B (Figure 4C). We also immunoblotted tumor samples with an α6B-specific Ab and observed that α6B is significantly higher in TPN samples (n = 17) compared to non-TPN (n = 18) and its expression is negatively correlated with ESRP1 (Figures 4D–4F).

VEGF/NRP/GLI1 Signaling Suppresses ESRP1 via BMI1

Based on the interesting negative correlation observed in tumor specimens between VEGF and ESRP1 expression, we investigated the possibility that VEGF signaling suppresses ESRP1 and, consequently, induces α6B expression. Previously, we reported that autocrine VEGF signaling, mediated through a neuropilin-2/α6β1 complex, promotes the initiation of TPN tumors via GLI1 (Goel et al., 2012a, 2013). In support of this possibility, we observed that cells expressing α6B (MDA-MB-435, MDA-MB-231, and SUM1315), as well as the MES cells, exhibited increased expression of VEGF, NRP1, and NRP2 compared to cells expressing α6A and the EPTH cells (Figures 5A and 5B). Inhibition of either VEGF (using small interfering RNA [siRNA]) or NRP (using an inhibitory peptide c-furSEMA) significantly reduced the self-renewal ability of the α6B transfectants (Figure 5C). Finally, depletion of VEGF caused a significant increase in ESRP1 and α6A expression but reduced α6B (Figure 5D).

Autocrine VEGF signaling has been shown to induce expression of GLI1 (Goel et al., 2013), a hedgehog target gene that has been implicated in the function of CSCs (Fiaschi et al., 2009; Goel et al., 2013; Liu et al., 2006). Indeed, we observed increased GLI1 expression in the MES population and α6B transfectants (Figures 5B and 5E). Importantly, GLI1 expression is significantly reduced by TALEN-mediated downregulation of α6B, supporting the role of α6Bβ1 in this VEGF/NRP/GLI1-signaling pathway (Figure 5F). Given that TALEN-mediated downregulation of α6B increased α6A and decreased GLI1, we hypothesized that GLI1 may inhibit ESRP1 expression. This hypothesis is supported by experiments in which we modulated GLI1 expression in SUM1315 and MCF-10A cells and observed a significant effect on ESRP1 expression (Figure 5G). We also detected a negative correlation between ESRP1 and GLI1 expression in a cohort of 310 breast cancer patients (p = 2.2 × 10^{-16}; Figure 5H) using cBIOPORTAL (http://cbioprotal.org; MSKCC). To substantiate the negative regulation of ESRP1 by GLI1, we analyzed mammary tumors in mouse mammary tumor virus (MMTV)-GLI1 and MMTV- polyoma virus middle T (PyV-MT) mice. Mammary tumors in MMTV-GLI1 mice have enhanced expression of VEGF, NRP2, and BMI-1 compared to MMTV-PyV-MT tumors (Goel et al., 2013). We detected reduced expression of ESRP1 and α6A and increased expression of α6B in MMTV-GLI1 compared to MMTV-PyV-MT tumors (Figure 5I).

To investigate how ESRP1 expression is inhibited by GLI1, we focused on BMI1 because GLI1 promotes breast CSC function by inducing BMI1 (Goel et al., 2013) and BMI1 functions as a transcriptional repressor (Bunker and Kingston, 1994; Goel et al., 2012b). Moreover, expression of GLI1 and BMI1 is significantly higher in the α6B transfectants and MES cells than in the
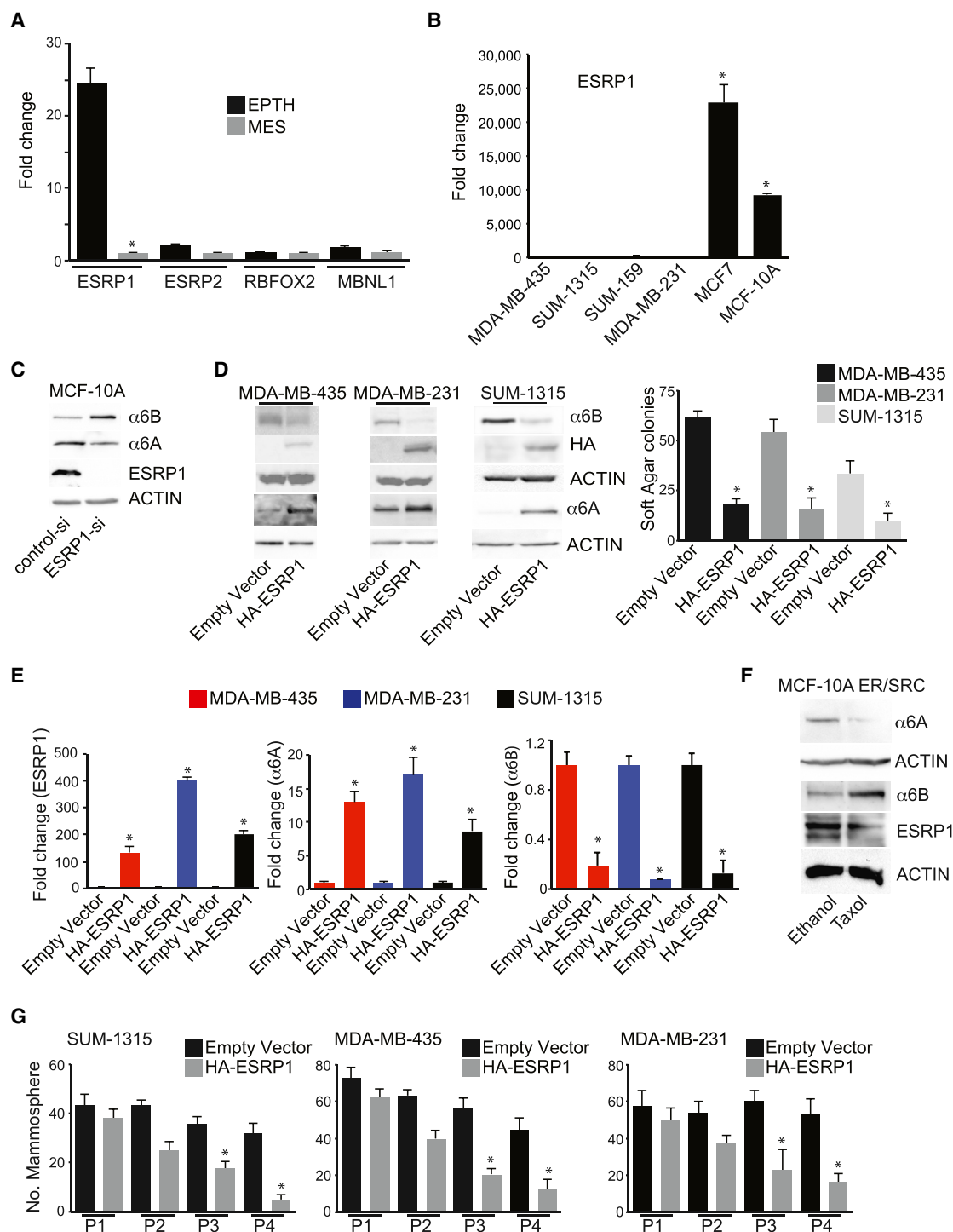
Figure 3. ESRP1 Promotes Integrin α6A Expression

(A) Expression of ESRP1, ESRP2, RBFOX2, and MBNL1 mRNAs was quantified in EPTH and MES cells using qPCR.

(B) Expression of ESRP1 mRNA was quantified in breast cancer cell lines using qPCR.

(C) ESRP1 was downregulated in MCF-10A cells, and cell extracts were immunoblotted to assess the expression of integrin subunits α6A, α6B, ESRP1, and actin.

(D) The effect of ESRP1 on α6B and α6A expression, as assessed by immunoblotting (left panels), or on the ability of breast cancer cell lines to form colonies in soft agar (right panel).

(legend continued on next page)

α6A transfectants and EPTH cells (Figures 6A and S4A). Exogenous expression of α6B in MCF7 cells increased GLI1 (Figure S4B) and BMI1 (Figure 6B), as well as their self-renewal ability and other established markers of stemness (Figures S4B and S4C). Expression of BMI1 in MCF-10A cells suppressed ESRP1 and α6A expression but increased α6B expression (Figure 6C). Conversely, downregulation of either BMI1 or GLI1 in MDA-MB-435 cells increased ESRP1 and α6A expression but reduced α6B expression (Figure 6D). We performed chromatin immunoprecipation (ChIP) to assess BMI1 binding to the ESRP1 promoter and observed binding to specific sequences within this promoter (Figure 6E). Self-renewal ability mediated by α6Bβ1 is dependent upon BMI1 because BMI1 downregulation inhibits the ability of α6B transfectants to form mammospheres in serial passage (Figure 6F). Finally, a negative correlation between BMI1 and ESRP1 was observed in our analysis of the human breast cancer data set described above (Figure 6G).

Collectively, our data indicate that autocrine VEGF signaling controls the splicing of the α6 integrin subunit by a mechanism that involves GLI1-mediated induction of BMI1 and BMI1-mediated repression of ESRP1. To validate this mechanism, we engineered MDA-MB-231 to express GFP under control of the VEGF promoter. FACS analysis revealed a small population of GFP+ cells (~1%) that expresses significantly higher levels of VEGF in comparison to the bulk population (Figure 7A). We isolated these populations and assessed their properties. These VEGF-high cells grow much more slowly (data not shown) and are more resistant to Taxol than the bulk population (Figure S5A). VEGF-high cells are unstable in culture, and they slowly become a mixture of VEGF-high and VEGF-low cells. In contrast, the VEGF-low population does not change in culture (data not shown). VEGF-high cells form more colonies in soft agar compared to VEGF-low cells, and colony formation is inhibited by VEGF downregulation in these cells (Figures 7B and S5B). VEGF-high, but not VEGF-low cells, are sensitive to VEGF and NRP inhibitors (Figure S5C), establishing the validity of this model system. Tumor onset upon orthotopic fat pad implantation, as well as self-renewal assays, indicate that VEGF-high cells are enriched for CSCs compared to VEGF-low cells (Figures 7C and 7D). Consistent with these findings, VEGF-high cells express high levels of α6B, NRPs, GLI1, and BMI1 but reduced levels of α6A and ESRP1 (Figures 7E and 7F). Finally, expression of ESRP1 in VEGF-high cells increased α6A expression (Figure 7G) but reduced self-renewal ability in vitro and tumor onset in vivo (Figures 7H and 7I). VEGF/GLI1 signaling also promotes chemoresistance because VEGF downregulation and GLI1 inhibition increased sensitivity to Taxol (Figure S5D).

DISCUSSION

This study revealed that the contribution of the α6β1 integrin to the function of breast CSCs is not dependent on its level of expression as often assumed but rather on the relative expression of a specific splice variant of this integrin, α6Bβ1. Conversely, the α6A integrins lack the ability to promote breast CSC function. The importance of α6Bβ1 is highlighted by our discovery that expression of the α6B subunit is repressed by the ESRP1-splicing factor and intimately associated with a VEGF autocrine signaling pathway that sustains CSCs and promotes tumor initiation. The fact that α6Bβ1 initiates a signaling pathway that sustains its expression argues for the existence of a feedforward loop involved in tumor initiation that has the α6Bβ1 splice variant at its nexus.

A major conclusion of this study is that the α6A and α6B cytoplasmic domains differ completely in their contribution to the function of CSCs. The realization that the α6 integrin subunit exists as two distinct variants that differ only in their cytoplasmic domains was made more than 20 years ago (Hogervorst et al., 1991; Tamura et al., 1991). Early studies focused primarily on correlating α6A and α6B expression with specific cell types and developmental stages (Hierck et al., 1993; Hogervorst et al., 1993). Interestingly, oncogenic transformation of keratinocytes was observed to increase α6B expression, but the functional consequences were not investigated (Tennenbaum et al., 1995). Mice that lack α6A, generated by removing the exon that encodes its cytoplasmic domain, developed normally and were characterized primarily by defects in lymphocyte migration (Gimond et al., 1998). More recently, α6A has been implicated in the proliferation of colon carcinoma cells (Groulx et al., 2014). We observed that downregulation of α6A did not impact mammosphere formation or α6B expression (Figure S5E). Together, these results support our hypothesis that α6B is the splice variant that is critical for slow-cycling stem cell function. In this context, it is worth noting that α6B expression had been associated with embryonic stem cells (Cooper et al., 1991; Tamura et al., 1991), but its functional contribution was not pursued. A major hindrance to the functional analysis of α6B had been the lack of an approach to target this variant specifically. RNAi is not feasible because of sequence homology between α6A and α6B. Specific function-blocking antibodies do not exist and could be difficult to generate. We were successful in circumventing these issues using gene-editing TALENs directed at the alternative splice site in the α6 subunit. This approach enabled us to inhibit α6B expression specifically and establish its contribution to CSCs.

Our data infer that α6Bβ1-mediated signaling is distinct from other α6 integrin signaling because it can promote the function of CSCs. This conclusion is supported by the finding that only α6Bβ1 has the ability to induce GLI1 and inhibit ESRP1 transcription. Interestingly, α6Bβ1 is a component of a VEGF signaling pathway that represses α6A and sustains α6B expression as evidenced by the fact that TALEN-mediated knockdown of α6B increases α6A expression and our previous finding that an α6β1/NRP2 complex mediates VEGF signaling (Goel et al.,

---

(E) The effect of ESRP1 expression on ESRP1 (left panels), integrin α6A expression (middle panel), or integrin α6B expression (right panel) was analyzed using qPCR.

(F) The CD44high/CD24low population from TAM-treated MCF-10A ER-SRC cells was treated with either Taxol or ethanol for 7 days, and expression of α6B, α6A, and ESRP1 was analyzed by immunoblotting.

(G) The effect of ESRP1 expression on self-renewal ability was analyzed by serial passage of mammospheres.
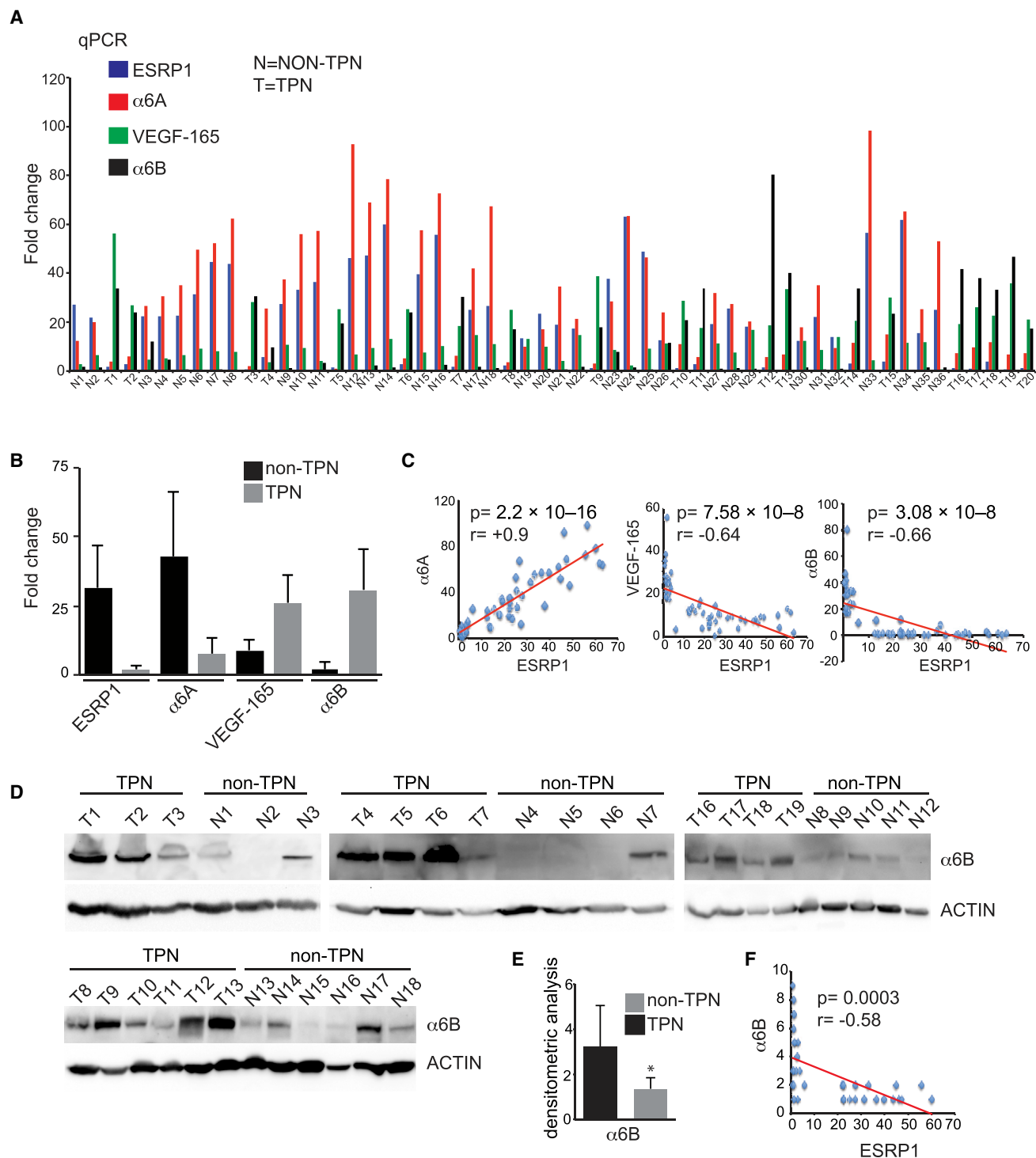
Figure 4. ESRP1 and Integrin α6A Expression Is Low in Triple-Negative Tumors and Negatively Correlated with Integrin α6B and VEGF

(A) Frozen clinical specimens from TPN (n = 20) and non-TPN (n = 36) breast tumors were used to compare ESRP1, integrin α6A, integrin α6B, and VEGF-165 by qPCR.

(B) Graph depicts the fold change in mRNA levels between the TPN and non-TPN specimens shown in (A).

(C) Correlation graphing reveals a significant positive correlation between α6A and ESRP1 expression (left panel), a significant negative correlation between VEGF-165 and ESRP1 expression (middle panel), and a significant negative correlation between α6B and ESRP1 expression (right panel).

(D) Frozen clinical specimens from TPN (n = 17) and non-TPN (n = 18) breast tumors were used to compare expression of integrin α6B by immunoblotting.

(E) Densitometric analysis of the immunoblot shown in (D).

(F) Correlation graphing reveals a significant negative correlation in the expression of integrin α6B and ESRP1.
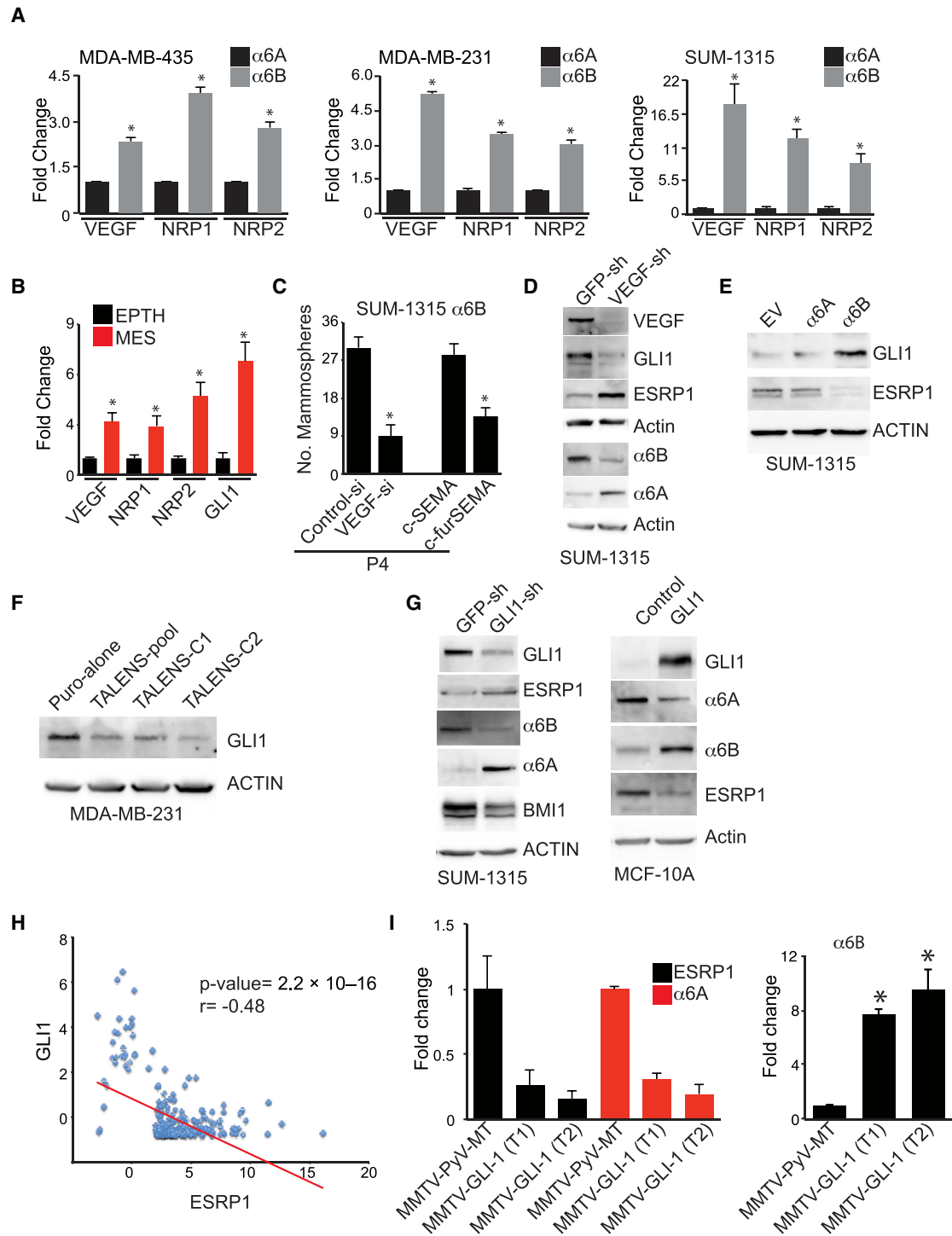
Figure 5. VEGF/NRP2/GLI1 Signaling Represses ESRP1 Expression and Promotes Integrin-α6Bβ1-Mediated Self-Renewal

(A) VEGF-A, NRP1, and NRP2 mRNA expression was quantified by qPCR in breast cancer cell lines expressing integrin α6A or α6B variants.

(B) EPTH and MES populations were analyzed for VEGF-A, NRP1, NRP2, or GLI1 mRNA expression using qPCR.

(C) SUM1315-α6B transfectants were depleted of VEGF and NRP using either VEGF siRNA or NRP inhibitors, and these cells were assayed for their ability to be passaged serially as mammospheres. The number of mammospheres observed at passage 4 is shown.

(D) VEGF was depleted in SUM1315 cells, and the expression of VEGF, GLI1, ESRP1, α6A, α6B, and actin was assessed by immunoblotting.

(E) Cell extracts from SUM1315 transfectants (EV, α6A, or α6B) were immunoblotted with Abs specific to GLI1, ESRP1, and actin.

(F) Expression of α6B was depleted in MDA-MB-231 cells using α6B-specific TALENs, and expression of GLI1 and actin was assessed by immunoblotting.
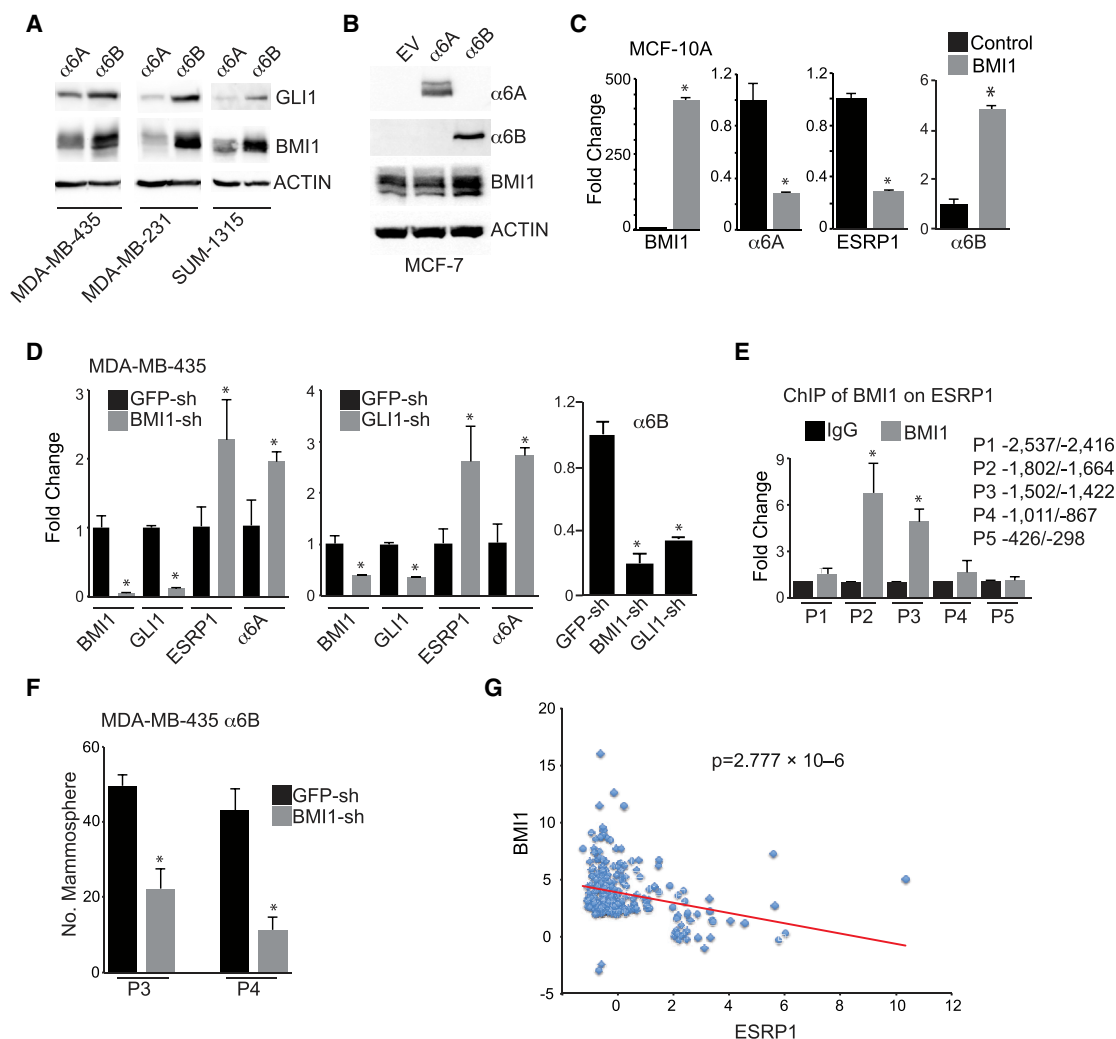
(legend continued on next page)

Figure 6. BMI1 Suppresses ESRP1 and Controls α6Bβ1-Mediated Self-Renewal
(A) Extracts from α6A- or α6B-expressing breast cancer cells were immunoblotted with Abs to GLI1, BMI1, and actin.
(B) MCF-7 cells expressing either EV, α6A, or α6B were analyzed for expression of α6A, α6B, BMI1, and actin.
(C) BMI1 was expressed in MCF-10A cells, and its effect on α6A, ESRP1, and α6B expression was assessed by qPCR.
(D) Downregulation of BMI1 or GLI1 significantly increased ESRP1 and α6A but reduced α6B mRNA levels.
(E) Binding of BMI1 on the ESRP1 promoter was analyzed using ChIP. Primers P2 and P3, which span the region −1,422 to −1,802 upstream of the transcription start site of ESRP1, show significant binding of BMI1. IgG, immunoglobulin.
(F) Effect of BMI1 downregulation on the self-renewal potential of α6B transfectants is shown at mammosphere passages 3 and 4.
(G) A significant negative correlation between expression of BMI1 and ESRP1 was observed in breast cancer patient cohorts.

2013). Also, α6B is the predominant variant observed in cells that exhibit autocrine VEGF/NRP2 signaling. These findings are significant because they provide a mechanism for how α6B expression is regulated in cancer. The limited data published on the α6 splice variants do not address how they are regulated differentially, especially in a pathophysiological context. In essence, our data support the existence of a feedforward signaling loop that involves α6Bβ1 and that functions to sustain α6B and repress α6A expression. Interestingly, a contribution of α6Bβ4 to this signaling pathway and the function of CSCs is not supported by our data despite the fact that α6β4 integrin has been implicated in breast cancer formation and progression (Guo et al., 2006; Lipscomb et al., 2005; Shaw et al., 1997). The MES population of CD44^{high}/CD24^{low} SRC-transformed

(G) Cell extracts from SUM1315 cells expressing either GFPsh or GLI1sh were immunoblotted using Abs to GLI1, ESRP1, α6A, α6B, BMI1, and actin (left panels). MCF-10A cells were transfected with GLI1 and analyzed for expression of GLI1, α6A, α6B, ESRP1, and actin (right panel).
(H) A significant negative correlation between GLI1 and ESRP1 expression was observed in breast cancer patient cohorts.
(I) Expression of ESRP1, α6A, and α6B is compared between MMTV-PyV-MT and MMTV-GLI1 mouse tumor models.
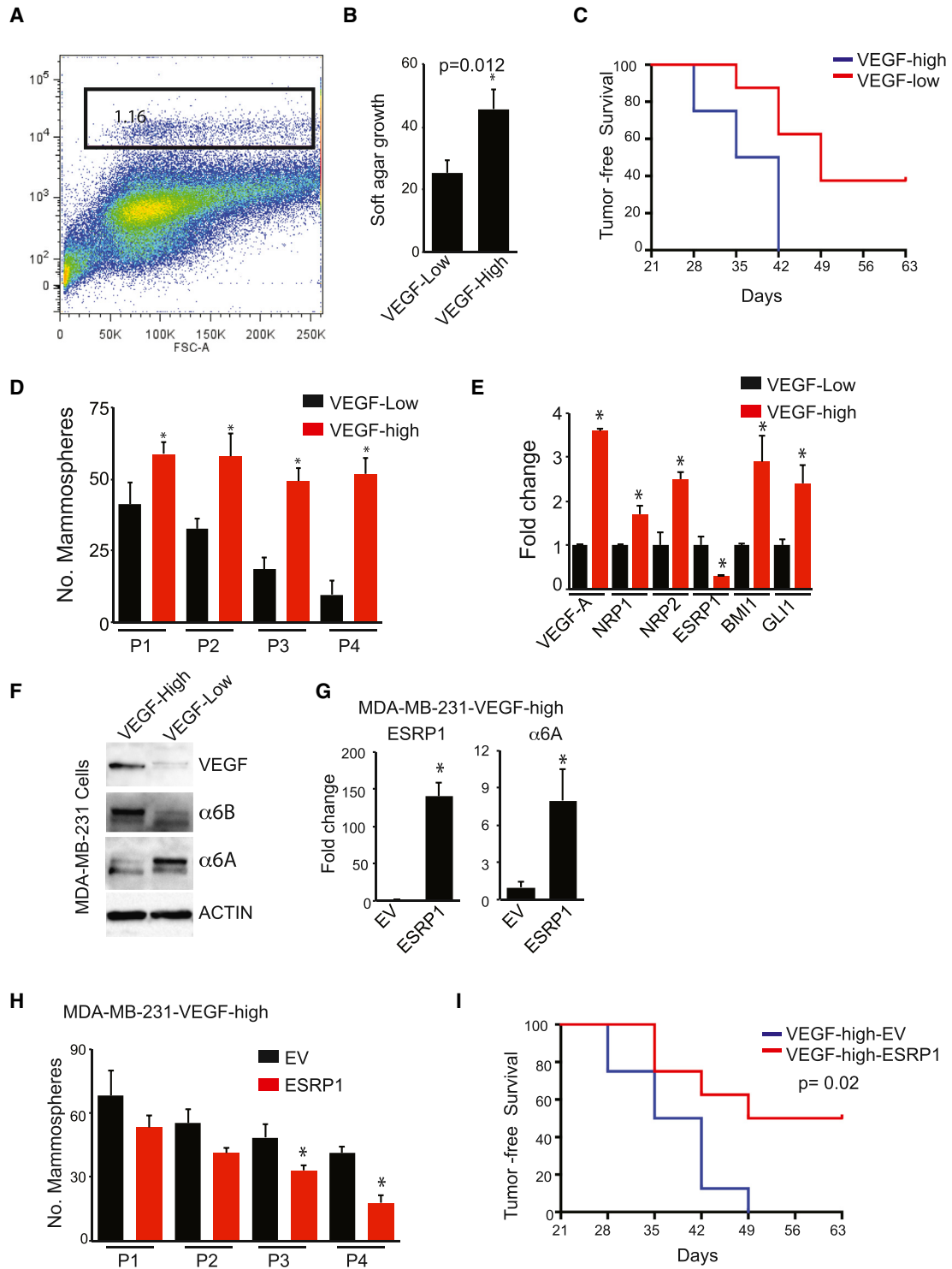
Figure 7. Integrin α6Bβ1 Is at the Nexus of a Feedforward VEGF-Signaling Loop that Sustains Self-Renewal and Tumor Initiation

(A) FACS profile of MDA-MB-231 cells stably expressing GFP under control of the VEGF promoter is shown.

(B) Freshly sorted VEGF-high or VEGF-low populations were used to measure colony formation in soft agar.

(C) VEGF-high or VEGF-low cells were implanted in the mammary fat pad of NSG mice (n = 8), and tumor formation was assessed by palpation. The curve comparison was done using log rank test (p = 0.008).

(D) The effect of VEGF expression on self-renewal ability was analyzed by serial passage of mammospheres.

(E) Expression of key signaling proteins in VEGF-high and VEGF-low cells was quantified by qPCR.

(legend continued on next page)

MCF-10A cells, which has stem cell properties, expresses very little β4 compared to the EPTH population (Figure 1D). This observation is consistent with the finding that β4 expression is repressed during the EMT (Yang et al., 2009). Moreover, late-passage mammospheres, which are enriched for CSCs, lack detectable β4 expression despite the fact that adherent cultures of the same cells express β4 (Figure S5F). The intriguing issue that arises from these observations is the mechanism by which α6β4 contributes to breast cancer formation (Guo et al., 2006; Lipscomb et al., 2005).

We conclude that the CD44^high/CD24^low population of cells enriched for CSCs in TPN breast cancer is actually comprised of distinct epithelial and mesenchymal subpopulations that differ markedly in stem cell properties and tumor-initiating potential. In this direction, a recent study observed heterogeneity in the tumor-initiating population of TPN breast cancer based on the level of CD24 expression (Azzam et al., 2013), substantiating the complexity of putative CSC populations and the need for more specific biomarkers. Our findings also bear on the current debate regarding the role of epithelial differentiation in the genesis of CSCs. Epithelial dedifferentiation and the EMT have been shown to have a causal role in the genesis of CSCs (Scheel et al., 2011; Scheel and Weinberg, 2012), and our data support the involvement of α6Bβ1 in this process. Nonetheless, recent studies have challenged this hypothesis and proposed that stem cell properties reside in an epithelial population (Ocaña et al., 2012; Sarrio et al., 2012). An advantage of our approach is that we were able to compare differentiated and dedifferentiated cells within the same population of cells enriched for stem cell makers and determine that their stem cell properties are manifested primarily in the dedifferentiated cells that are characterized by a high ratio of α6B/α6A and expression of mesenchymal markers. Nonetheless, the epithelial subpopulation of CD44^high/CD24^low cells harbors some stem cell properties as evidenced by the data in Figure 1I, and we are intrigued by the possibility that this population may facilitate the function of the mesenchymal population. It is also worth noting that CSC properties differ among cancers and cancer subtypes (Visvader and Lindeman, 2012) and that our findings are relevant to TPN breast cancer.

We conclude from our data that autocrine VEGF signaling promotes CSC function by regulating the expression of splicing factors that contribute to posttranscriptional gene regulation. This conclusion establishes a connection between autocrine growth factor signaling and RNA splicing. Our data also impact the emerging importance of alternative RNA splicing to the EMT and stem cell biology (Brown et al., 2011; De Craene and Berx, 2013; Han et al., 2013; Shapiro et al., 2011; Warzecha et al., 2010; Yae et al., 2012). Epithelial cells harbor a complex, alternative splicing network that contributes to the expression of splice variants of key proteins that sustain the epithelial

phenotype (Warzecha et al., 2010). The regulated expression of splicing factors such as the ESRPs enables the expression of specific splice variants in epithelial cells. Alterations in the expression of splicing factors can disrupt epithelial splicing, resulting in an EMT (Brown et al., 2011; Shapiro et al., 2011; Warzecha et al., 2010) and contributing to the genesis of CSCs (Yae et al., 2012). An important observation from our perspective is that loss of ESRP1 expression, which occurs during the EMT, causes an increase in α6B and a decrease in α6A expression, a finding that implicates this splicing factor in the genesis of α6Bβ1 (Warzecha et al., 2010). More specifically, it has been shown that ESRP1 binds to a specific UGG-rich recognition motif in the α6 mRNA and promotes exon inclusion to generate α6A (Warzecha et al., 2010). Loss of ESRP1 results in the deletion of this exon from the mature mRNA and the consequent generation of α6B and diminution of α6A. The importance of our work is that we established that autocrine VEGF signaling sustains BMI1-mediated repression of ESRP1 and the consequent increase in α6B and decrease in α6A expression. This finding is significant because it establishes an integrated signaling pathway that regulates integrin splicing. Also, autocrine VEGF signaling is emerging as a critical pathway that drives CSC function and tumor initiation, but the mechanisms involved are still being elucidated (Beck et al., 2011; Goel et al., 2012b, 2013; Goel and Mercurio, 2013; Lichtenberger et al., 2010). Clearly, the involvement of RNA splicing adds a dimension to the mechanism by which autocrine VEGF signaling contributes to tumor initiation.

We propose that the ratio of α6B to α6A integrin subunit expression is more indicative of stem cell phenotype than total α6 expression, at least for TPN breast cancer. This conclusion is timely and significant for several reasons. Although high α6 (CD49f) expression is often used as a marker to identify breast and other CSCs (Cariati et al., 2008; Lathia et al., 2010; Meyer et al., 2010; Vieira et al., 2012), other studies on breast CSCs have observed a decrease in α6 expression (Vaillant et al., 2008). Based on our findings, we suggest that this discrepancy reflects differences in the relative expression of α6A and α6B. In fact, we observed a marked decrease in overall α6 expression in the MES population of CD44^high/CD24^low cells compared to the EPTH population (Figure 1D) but a significant increase in α6B. Given the heterogeneity that exists within CSC populations based on our studies and others (Azzam et al., 2013), α6B expression could be used as a biomarker to define CSCs more rigorously. The translational impact of our findings could be significant. High α6B expression in primary tumors could be prognostic for poor outcome and it could also be used to monitor the efficacy of therapy in patients with TPN breast cancer. Finally, therapeutic approaches that target the splicing proteins involved in the genesis of α6B or the signaling pathway that sustains its expression could be effective for the treatment of

(F) Expression of VEGF, α6A, and α6B in VEGF-high and low populations was assessed by immunoblotting. VEGF-high cells express high levels of α6B and low levels of α6A compared to the VEGF-low population.

(G) ESRP1 expression in the VEGF-high population increases α6A mRNA expression as measured by qPCR.

(H) Effect of ESRP1 expression on the self-renewal ability of VEGF-high cells was analyzed by serial passaging of mammospheres.

(I) Effect of ESRP1 expression in VEGF-high cells on tumor onset was analyzed by transplanting transfectants (10^5 cells/mouse) in mammary fat pads of NSG mice (n = 8). The curve comparison was done using log rank test (p = 0.02).

TPN and other drug-resistant breast cancers that are enriched with CSCs (Calcagno et al., 2010).

EXPERIMENTAL PROCEDURES

Reagents and Antibodies

Matrigel was purchased from BD Biosciences; Taxol and 4-hydroxytamoxifen (TAM) were purchased from Sigma-Aldrich. The following Abs were used: α6 (AA6A, provided by Anne Cress; GoH3, purchased from Millipore); α6A (1A10; Millipore); α6B (6B4; Millipore); N-cadherin (Invitrogen); E-cadherin (Invitrogen); tubulin (Sigma-Aldrich); HIF-1α (Novus Biologicals); ESRP1 (Sigma-Aldrich); actin (Sigma-Aldrich); tubulin (Sigma-Aldrich); hemagglutinin (HA) (Roche); GLI1 (Cell Signaling); BMI-1 (Cell Signaling); cytokeratin 8/cytokeratin 18 (Novacastra); phycoerythrin-conjugated anti-CD44 (BD Bioscience); Alexa Fluor 647 anti-CD24 (BD Bioscience); and VEGF (Calbiochem). A NRP-blocking peptide (c-furSEMA) was provided by Dr. C. Vander Kooi (University of Kentucky), and bevacizumab was obtained as described (Goel et al., 2013).

Primary Breast Tumors

Human breast tissues were obtained in compliance with the Institutional Review Board of the University of Massachusetts Medical School. Snap-frozen tumors were homogenized to isolate either RNA or protein. For quantitative PCR (qPCR), RNA was isolated using RNeasy kit (QIAGEN) and converted to cDNA using Transcriptor First Strand cDNA Synthesis kit (Roche). We performed qPCR with a SYBR Green PCR master mix using an ABI Prism 7900HT instrument (Applied Biosystems). Sequences for primers used are provided in Figure S6. Tumor extracts were also immunoblotted to detect expression of α6B integrin or actin.

Cells

SUM1315 and SUM159 cells were provided by Dr. Steve Ethier (Medical College of South Carolina). MCF-10A cells were obtained from the Barbara Ann Karmanos Cancer Institute. ER-SRC-transformed MCF-10A cells were provided by Dr. Kevin Struhl (Harvard Medical School). MDA-MB-231, MDA-MB-435, MCF7, SK-BR-3, and T-47D cells were obtained from American Type Culture Collection.

Molecular Reagents

Lentiviral constructs containing shRNAs specific for α6 integrin (TRCN0000296162), GLI1 (TRCN0000020484), ESRP1 (TRCN0000240875), or GFP (RHS4459) were obtained from Open Biosystems. An siRNA–SMARTpool to ESRP1 (L-020672-01-0005) was purchased from Thermo Fisher Scientific. A lentiviral plasmid (FUGW) expressing BMI-1 was obtained from Addgene. HA-ESRP1 constructs were provided by Dr. Chonghui Cheng (Northwestern University). pRC-α6A or α6B plasmids were prepared as described (Shaw et al., 1993) and subcloned into the lentiviral vector pCDH. A wild-type GLI1 construct was provided by Dr. Junhao Mao (UMASS Medical School). TALENs that target the splicing site for α6B were designed by the UMASS Core facility. The donor plasmid was prepared by cloning 500 bp upstream of the TALENs target site (left arm) followed by SV40 enhancer plus promoter fragment, puromycin coding sequence, and then 500 bp downstream of the TALENs target site (right arm). Upon recombination, the puromycin gene along with its promoter plus enhancer region were inserted at the α6B-splicing site. The sequence of TALENs is provided in Figure S6. We used an obligate heterodimer vector to avoid hits to the tal1-tal1 or tal2-tal2 sites. The plasmid expressing GFP under VEGF-A promoter was constructed by replacing the CMV promoter from pEGFP-N1 vector with the promoter region (−2,414 to −79) of human VEGF-A in the forward direction.

Cell-Based Assays

Flow cytometry was used to analyze surface expression of the α6 integrin, CD44, and CD24 in breast cancer cell lines. PKH-26 staining was performed as per manufacturer's instructions (Sigma). Mammosphere and ChIP assays were performed as described (Goel et al., 2012b, 2013). ChIP experiments were performed at least thrice, and the variation was less than 20%. The primers used to amplify the ESRP1 promoter are provided in Figure S6.

Immunoblotting and qPCR

Cells were extracted in either a Triton X-100 buffer (1% Triton X-100, 150 mM NaCl, 50 mM Tris-HCl [pH 7.5], 1 mM phenylmethanesulfonylfluoride [PMSF], and protease inhibitors) or RIPA (50 mM Tris-HCl [pH 7.4], 150 mM NaCl, 0.1% SDS, 0.5% sodium deoxycholate, 1 mM PMSF, and protease inhibitors). The proteins were separated by SDS-PAGE and immunoblotted using Abs as specified in the figure legends. For qPCR, RNA was isolated and qPCR was performed. Sequences for primers used are provided in Figure S6. Primers for α6B mRNA quantitation were custom synthesized as described (Groulx et al., 2014).

Xenograft Experiments

MDA-MB-435 or SUM1315 transfectants expressing α6A or α6B were mixed with Matrigel at a 10-fold dilution and injected into a mammary fat pad of immunocompromised NSG mice. Tumor onset was determined by palpation. In some experiments, cells (10^6) were injected into a mammary fat pad of NSG mice and tumor onset was determined by palpation.

Transgenic Mice

MMTV-PyV-MT mice transgenic for the PyV-MT antigen under the control of the MMTV promoter (Jackson Laboratory) were generated as described (Nagle et al., 2004). The MMTV-GLI1 transgenic mouse model was generated previously (Fiaschi et al., 2009). These mice express transgenic GLI1 in the presence of doxycycline, which was added to drinking water with 5% sucrose. RNA was isolated from the tumors collected from these mice. All animal experiments were in accordance with institutional guidelines and are approved by Institutional Animal Care and Use Committees.

Statistical Analysis

Statistical analysis (mean, Student's t test, correlation, and ANOVA) was performed with R version 3.0.1 (Figure S7).

SUPPLEMENTAL INFORMATION

Supplemental Information includes Supplemental Experimental Procedures and seven figures and can be found with this article online at http://dx.doi.org/10.1016/j.celrep.2014.03.059.

REFERENCES

Al-Hajj, M., Wicha, M.S., Benito-Hernandez, A., Morrison, S.J., and Clarke, M.F. (2003). Prospective identification of tumorigenic breast cancer cells. Proc. Natl. Acad. Sci. USA 100, 3983–3988.

Azzam, D.J., Zhao, D., Sun, J., Minn, A.J., Ranganathan, P., Drews-Elger, K., Han, X., Picon-Ruiz, M., Gilbert, C.A., Wander, S.A., et al. (2013). Triple negative breast cancer initiating cell subsets differ in functional and molecular characteristics and in γ-secretase inhibitor drug responses. EMBO Mol Med 5, 1502–1522.

Baccelli, I., and Trumpp, A. (2012). The evolving concept of cancer and metastasis stem cells. J. Cell Biol. *198*, 281–293.

Beck, B., Driessens, G., Goossens, S., Youssef, K.K., Kuchnio, A., Caauwe, A., Sotiropoulou, P.A., Loges, S., Lapouge, G., Candi, A., et al. (2011). A vascular niche and a VEGF-Nrp1 loop regulate the initiation and stemness of skin tumours. Nature *478*, 399–403.

Brown, R.L., Reinke, L.M., Damerow, M.S., Perez, D., Chodosh, L.A., Yang, J., and Cheng, C. (2011). CD44 splice isoform switching in human and mouse epithelium is essential for epithelial-mesenchymal transition and breast cancer progression. J. Clin. Invest. *121*, 1064–1074.

Bunker, C.A., and Kingston, R.E. (1994). Transcriptional repression by Drosophila and mammalian Polycomb group proteins in transfected mammalian cells. Mol. Cell. Biol. *14*, 1721–1732.

Calcagno, A.M., Salcido, C.D., Gillet, J.P., Wu, C.P., Fostel, J.M., Mumau, M.D., Gottesman, M.M., Varticovski, L., and Ambudkar, S.V. (2010). Prolonged drug selection of breast cancer cells and enrichment of cancer stem cell characteristics. J. Natl. Cancer Inst. *102*, 1637–1652.

Cariati, M., Naderi, A., Brown, J.P., Smalley, M.J., Pinder, S.E., Caldas, C., and Purushotham, A.D. (2008). Alpha-6 integrin is necessary for the tumourigenicity of a stem cell-like subpopulation within the MCF7 breast cancer cell line. Int. J. Cancer *122*, 298–304.

Cooper, H.M., Tamura, R.N., and Quaranta, V. (1991). The major laminin receptor of mouse embryonic stem cells is a novel isoform of the alpha 6 beta 1 integrin. J. Cell Biol. *115*, 843–850.

De Craene, B., and Berx, G. (2013). Regulatory networks defining EMT during cancer initiation and progression. Nat. Rev. Cancer *13*, 97–110.

Dean, M., Fojo, T., and Bates, S. (2005). Tumour stem cells and drug resistance. Nat. Rev. Cancer *5*, 275–284.

Douville, J., Beaulieu, R., and Balicki, D. (2009). ALDH1 as a functional marker of cancer stem and progenitor cells. Stem Cells Dev. *18*, 17–25.

Fiaschi, M., Rozell, B., Bergström, A., and Toftgård, R. (2009). Development of mammary tumors by conditional expression of GLI1. Cancer Res. *69*, 4810–4817.

Gimond, C., Baudoin, C., van der Neut, R., Kramer, D., Calafat, J., and Sonnenberg, A. (1998). Cre-loxP-mediated inactivation of the alpha6A integrin splice variant in vivo: evidence for a specific functional role of alpha6A in lymphocyte migration but not in heart development. J. Cell Biol. *143*, 253–266.

Goel, H.L., and Mercurio, A.M. (2013). VEGF targets the tumour cell. Nat. Rev. Cancer *13*, 871–882.

Goel, H.L., Pursell, B., Standley, C., Fogarty, K., and Mercurio, A.M. (2012a). Neuropilin-2 regulates α6β1 integrin in the formation of focal adhesions and signaling. J. Cell Sci. *125*, 497–506.

Goel, H.L., Chang, C., Pursell, B., Leav, I., Lyle, S., Xi, H.S., Hsieh, C.C., Adisetiyo, H., Roy-Burman, P., Coleman, I.M., et al. (2012b). VEGF/neuropilin-2 regulation of Bmi-1 and consequent repression of IGF-IR define a novel mechanism of aggressive prostate cancer. Cancer Discov. *2*, 906–921.

Goel, H.L., Pursell, B., Chang, C., Shaw, L.M., Mao, J., Simin, K., Kumar, P., Vander Kooi, C.W., Shultz, L.D., Greiner, D.L., et al. (2013). GLI1 regulates a novel neuropilin-2/α6β1 integrin based autocrine pathway that contributes to breast cancer initiation. EMBO Mol Med *5*, 488–508.

Groulx, J.F., Giroux, V., Beauséjour, M., Boudjadi, S., Basora, N., Carrier, J.C., and Beaulieu, J.F. (2014). Integrin α6A splice variant regulates proliferation and the Wnt/β-catenin pathway in human colorectal cancer cells. Carcinogenesis, Published online February 6, 2014. http://dx.doi.org/10.1093/carcin/bgu006.

Guo, W., Pylayeva, Y., Pepe, A., Yoshioka, T., Muller, W.J., Inghirami, G., and Giancotti, F.G. (2006). Beta 4 integrin amplifies ErbB2 signaling to promote mammary tumorigenesis. Cell *126*, 489–502.

Han, H., Irimia, M., Ross, P.J., Sung, H.K., Alipanahi, B., David, L., Golipour, A., Gabut, M., Michael, I.P., Nachman, E.N., et al. (2013). MBNL proteins repress ES-cell-specific alternative splicing and reprogramming. Nature *498*, 241–245.

Hierck, B.P., Thorsteinsdóttir, S., Niessen, C.M., Freund, E., Iperen, L.V., Feyen, A., Hogervorst, F., Poelmann, R.E., Mummery, C.L., and Sonnenberg, A. (1993). Variants of the alpha 6 beta 1 laminin receptor in early murine development: distribution, molecular cloning and chromosomal localization of the mouse integrin alpha 6 subunit. Cell Adhes. Commun. *1*, 33–53.

Hogervorst, F., Kuikman, I., van Kessel, A.G., and Sonnenberg, A. (1991). Molecular cloning of the human alpha 6 integrin subunit. Alternative splicing of alpha 6 mRNA and chromosomal localization of the alpha 6 and beta 4 genes. Eur. J. Biochem. *199*, 425–433.

Hogervorst, F., Admiraal, L.G., Niessen, C., Kuikman, I., Janssen, H., Daams, H., and Sonnenberg, A. (1993). Biochemical characterization and tissue distribution of the A and B variants of the integrin alpha 6 subunit. J. Cell Biol. *121*, 179–191.

Iliopoulos, D., Hirsch, H.A., Wang, G., and Struhl, K. (2011). Inducible formation of breast cancer stem cells and their dynamic equilibrium with non-stem cancer cells via IL6 secretion. Proc. Natl. Acad. Sci. USA *108*, 1397–1402.

Lathia, J.D., Gallagher, J., Heddleston, J.M., Wang, J., Eyler, C.E., Macswords, J., Wu, Q., Vasanji, A., McLendon, R.E., Hjelmeland, A.B., and Rich, J.N. (2010). Integrin alpha 6 regulates glioblastoma stem cells. Cell Stem Cell *6*, 421–432.

Lichtenberger, B.M., Tan, P.K., Niederleithner, H., Ferrara, N., Petzelbauer, P., and Sibilia, M. (2010). Autocrine VEGF signaling synergizes with EGFR in tumor cells to promote epithelial cancer development. Cell *140*, 268–279.

Lipscomb, E.A., Simpson, K.J., Lyle, S.R., Ring, J.E., Dugan, A.S., and Mercurio, A.M. (2005). The alpha6beta4 integrin maintains the survival of human breast carcinoma cells in vivo. Cancer Res. *65*, 10970–10976.

Liu, S., Dontu, G., Mantle, I.D., Patel, S., Ahn, N.S., Jackson, K.W., Suri, P., and Wicha, M.S. (2006). Hedgehog signaling and Bmi-1 regulate self-renewal of normal and malignant human mammary stem cells. Cancer Res. *66*, 6063–6071.

Mercurio, A.M. (1990). Laminin: multiple forms, multiple receptors. Curr. Opin. Cell Biol. *2*, 845–849.

Meyer, M.J., Fleming, J.M., Lin, A.F., Hussnain, S.A., Ginsburg, E., and Vonderhaar, B.K. (2010). CD44posCD49fhiCD133/2hi defines xenograft-initiating cells in estrogen receptor-negative breast cancer. Cancer Res. *70*, 4624–4633.

Nagle, J.A., Ma, Z., Byrne, M.A., White, M.F., and Shaw, L.M. (2004). Involvement of insulin receptor substrate 2 in mammary tumor metastasis. Mol. Cell. Biol. *24*, 9726–9735.

Nieto, M.A., and Cano, A. (2012). The epithelial-mesenchymal transition under control: global programs to regulate epithelial plasticity. Semin. Cancer Biol. *22*, 361–368.

Ocaña, O.H., Córcoles, R., Fabra, A., Moreno-Bueno, G., Acloque, H., Vega, S., Barrallo-Gimeno, A., Cano, A., and Nieto, M.A. (2012). Metastatic colonization requires the repression of the epithelial-mesenchymal transition inducer Prrx1. Cancer Cell *22*, 709–724.

Pece, S., Tosoni, D., Confalonieri, S., Mazzarol, G., Vecchi, M., Ronzoni, S., Bernard, L., Viale, G., Pelicci, P.G., and Di Fiore, P.P. (2010). Biological and molecular heterogeneity of breast cancers correlates with their cancer stem cell content. Cell *140*, 62–73.

Pinto, C.A., Widodo, E., Waltham, M., and Thompson, E.W. (2013). Breast cancer stem cells and epithelial mesenchymal plasticity - Implications for chemoresistance. Cancer Lett. *341*, 56–62.

Sarrio, D., Franklin, C.K., Mackay, A., Reis-Filho, J.S., and Isacke, C.M. (2012). Epithelial and mesenchymal subpopulations within normal basal breast cell lines exhibit distinct stem cell/progenitor properties. Stem Cells *30*, 292–303.

Scheel, C., and Weinberg, R.A. (2012). Cancer stem cells and epithelial-mesenchymal transition: concepts and molecular links. Semin. Cancer Biol. *22*, 396–403.

Scheel, C., Eaton, E.N., Li, S.H., Chaffer, C.L., Reinhardt, F., Kah, K.J., Bell, G., Guo, W., Rubin, J., Richardson, A.L., and Weinberg, R.A. (2011). Paracrine and autocrine signals induce and maintain mesenchymal and stem cell states in the breast. Cell *145*, 926–940.

Shapiro, I.M., Cheng, A.W., Flytzanis, N.C., Balsamo, M., Condeelis, J.S., Oktay, M.H., Burge, C.B., and Gertler, F.B. (2011). An EMT-driven alternative

splicing program occurs in human breast cancer and modulates cellular phenotype. PLoS Genet. *7*, e1002218.

Shaw, L.M., Lotz, M.M., and Mercurio, A.M. (1993). Inside-out integrin signaling in macrophages. Analysis of the role of the alpha 6A beta 1 and alpha 6B beta 1 integrin variants in laminin adhesion by cDNA expression in an alpha 6 integrin-deficient macrophage cell line. J. Biol. Chem. *268*, 11401–11408.

Shaw, L.M., Rabinovitz, I., Wang, H.H., Toker, A., and Mercurio, A.M. (1997). Activation of phosphoinositide 3-OH kinase by the alpha6beta4 integrin promotes carcinoma invasion. Cell *91*, 949–960.

Tamura, R.N., Cooper, H.M., Collo, G., and Quaranta, V. (1991). Cell type-specific integrin variants with alternative alpha chain cytoplasmic domains. Proc. Natl. Acad. Sci. USA *88*, 10183–10187.

Tanei, T., Morimoto, K., Shimazu, K., Kim, S.J., Tanji, Y., Taguchi, T., Tamaki, Y., and Noguchi, S. (2009). Association of breast cancer stem cells identified by aldehyde dehydrogenase 1 expression with resistance to sequential Pacli-taxel and epirubicin-based chemotherapy for breast cancers. Clin. Cancer Res. *15*, 4234–4241.

Tennenbaum, T., Belanger, A.J., Glick, A.B., Tamura, R., Quaranta, V., and Yuspa, S.H. (1995). A splice variant of alpha 6 integrin is associated with malignant conversion in mouse skin tumorigenesis. Proc. Natl. Acad. Sci. USA *92*, 7041–7045.

Vaillant, F., Asselin-Labat, M.L., Shackleton, M., Forrest, N.C., Lindeman, G.J., and Visvader, J.E. (2008). The mammary progenitor marker CD61/beta3 integrin identifies cancer stem cells in mouse models of mammary tumorigenesis. Cancer Res. *68*, 7711–7717.

Vieira, A.F., Ricardo, S., Ablett, M.P., Dionísio, M.R., Mendes, N., Albergaria, A., Farnie, G., Gerhard, R., Cameselle-Teijeiro, J.F., Seruca, R., et al. (2012). P-cadherin is coexpressed with CD44 and CD49f and mediates stem cell properties in basal-like breast cancer. Stem Cells *30*, 854–864.

Visvader, J.E., and Lindeman, G.J. (2012). Cancer stem cells: current status and evolving complexities. Cell Stem Cell *10*, 717–728.

Warzecha, C.C., Jiang, P., Amirikian, K., Dittmar, K.A., Lu, H., Shen, S., Guo, W., Xing, Y., and Carstens, R.P. (2010). An ESRP-regulated splicing programme is abrogated during the epithelial-mesenchymal transition. EMBO J. *29*, 3286–3300.

Yae, T., Tsuchihashi, K., Ishimoto, T., Motohara, T., Yoshikawa, M., Yoshida, G.J., Wada, T., Masuko, T., Mogushi, K., Tanaka, H., et al. (2012). Alternative splicing of CD44 mRNA by ESRP1 enhances lung colonization of metastatic cancer cell. Nat Commun *3*, 883.

Yang, X., Pursell, B., Lu, S., Chang, T.K., and Mercurio, A.M. (2009). Regulation of beta 4-integrin expression by epigenetic modifications in the mammary gland and during the epithelial-to-mesenchymal transition. J. Cell Sci. *122*, 2473–2480.